ECE 445

SENIOR DESIGN LABORATORY

PROJECT PROPOSAL

Design Document for ECE 445: Terrain-adaptive bipedal service robot

---

Team #2

YUAN ZHOU
(yuanz15@illinois.edu)
ZIHAO YE
(zihaoye5@illinois.edu)
BINHAO WANG
(binhaow2@illinois.edu)
GAOKAI ZHANG
(gaokaiz2@illinois.edu)

TA: Xinlei Chang

April 13, 2025

Abstract

This project describes the design and creation of a service robot that is bipedal and capable of navigating across uneven and complex surfaces. The robotic vehicle is intended to enhance mobility in environments that traditional wheeled robots have a hard time dealing with, such as stairs, slopes, and rough outdoor areas. Using feedback from realtime sensors, modular mechanical components, and a reinforcement learning-based motion controller, the robot guarantees consistent and efficient movement. Key attributes include obstacle detection, dynamic balancing, and a user-friendly interface that is designed to be integrated with human intelligence. The project focuses on safety and ethical concerns, including the protection of privacy, the security of data, and environmentally responsible design decisions. By providing dependable, autonomous assistance in both domestic and professional settings, this dual-legged robot provides novel solutions to service problems in human-oriented environments.

Contents

List of Figures

List of Tables

1 Introduction

We are developing a well-rounded **terrain-adaptive bipedal robot** which is specifically engineered to smoothly and efficiently navigate diverse and challenging terrains including but not limited to uneven grounds like staircases, slopes, and outdoor areas where unpredictable surfaces may occur.

This document outlines our project's overall problem-solution overview, background rationale, core functionalities, along with the overall benefits, distinctive technical features, and essential performance benchmarks which are required for successful implementation and practical utility.

1.1 Background and Problem-Solution Overview

Legged robotic systems, particularly bipedal platforms, are increasingly recognized for their potential to overcome the limitations of wheeled and tracked robots in unstructured environments. Unlike wheeled systems that rely on flat, continuous terrain, bipedal robots can traverse complex features such as stairs, debris, and narrow corridors. However, real-world deployment remains constrained by difficulties in achieving robust, adaptive, and real-time control. Advances in quadrupedal systems—such as the MIT Cheetah 3 and Mini Cheetah—have demonstrated the efficacy of convex model predictive control (MPC) in delivering dynamic and robust locomotion under challenging conditions [1]–[3]. Parallel efforts in humanoid robotics have proposed centroidal dynamics-based whole-body controllers, which enhance both locomotion and manipulation by improving coordination and dynamic balance [4], [5]. Yet, few of these approaches generalize effectively to bipedal systems—particularly compact or low-cost platforms—due to high complexity, expensive actuation, and limited learning-based adaptability.

To address this gap, our project introduces a compact terrain-adaptive bipedal robot that integrates reinforcement learning-based control, proprioceptive feedback, and a streamlined mechanical architecture. Rather than relying on high-fidelity models or costly hardware, our system prioritizes adaptive learning for gait generation and real-time control. Drawing inspiration from centroidal momentum regulation in humanoid systems [4] and unified MPC frameworks for whole-body mobility [5], we combine the predictive power of MPC-style control with the flexibility of reinforcement learning. This hybrid approach enables dynamic gait switching, real-time terrain response, and stable locomotion across a range of environments. Our robot aims to lower the barrier to entry for bipedal locomotion research, offering a scalable and cost-effective platform for academic and applied use cases where adaptability and autonomy are critical.

1.2 Visual Aid

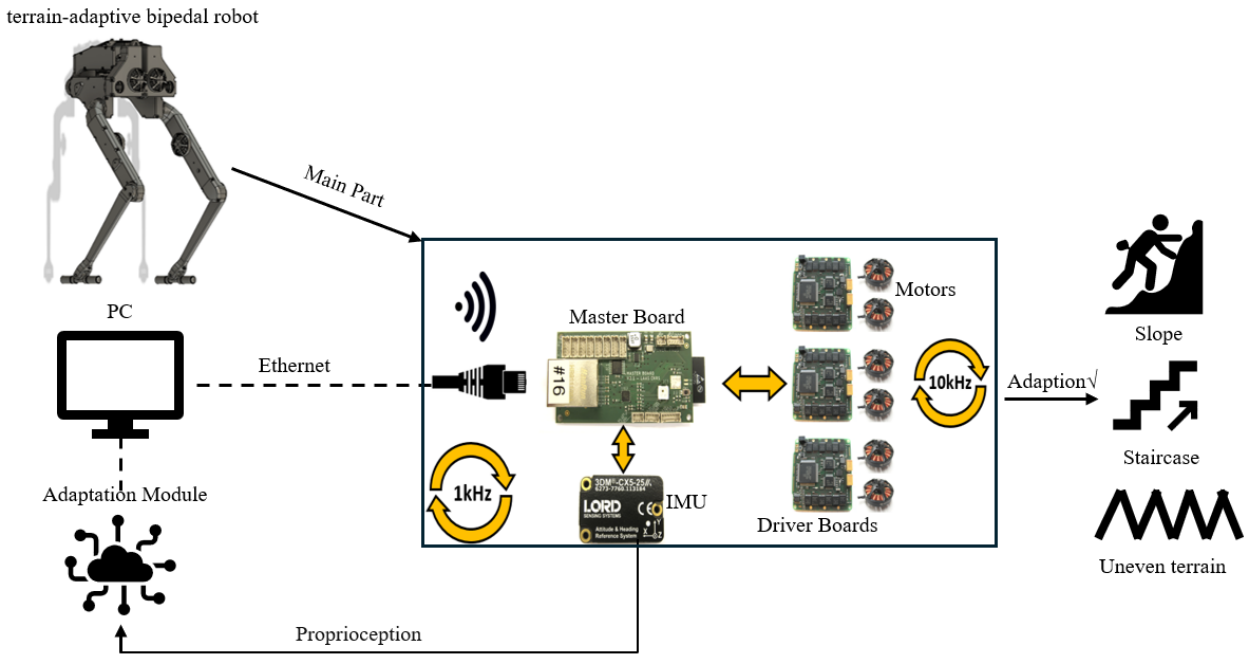

Figure 1: Visual aid of our project.

1.3 High-Level Requirements

- **Mobility Performance:** The robot must reliably and stably traverse obstacles including steps up to 10 cm high and slopes of up to 15° inclination without losing balance.
- **Low Latency Control:** All sensor processing and control communications must maintain a latency below 10 ms to ensure responsive and accurate control.
- **Impact Resilience:** The robot must effectively handle dynamic impacts and disturbances up to 10 N, maintaining stability and operational consistency.

1.4 Functions

- Capability to execute stable, adaptive walking patterns across diverse terrains including stairs, uneven grounds, and outdoor surfaces.
- Advanced real-time obstacle detection and autonomous avoidance mechanisms.
- Intuitive, user-friendly interface for straightforward control, monitoring, and interaction.
- Highly modular and expandable design, supporting easy customization and adaptability.

1.5 Benefits

This terrain-adaptive bipedal robot significantly enhances safety and reduces the physical effort required in difficult environments. Its well-designed components allow it to move through narrow or crowded spaces where wheeled and non-adaptive legged robots may fail. Future upgrades could enable the robot to perform tasks such as transporting objects, navigating hazardous environments, and providing consistent service in household and industrial contexts. These capabilities promise to improve operational efficiency, convenience, and safety.

1.6 Features

- **All-Terrain Mobility:** Capable of adapting to varied terrains including gravel, carpet, stairs, inclines, and other complex environments.
- **Dynamic Stability:** Robust mechanisms for maintaining balance and quickly recovering from disturbances or impacts.
- **Safe Interaction:** Integrated obstacle detection technologies for safe, collision-free operation near humans.
- **Ease of Use:** An intuitive interface that is accessible even to non-technical users.
- **Expandable and Modular:** A flexible design that allows easy integration and upgrading of components and functions.

2 Design

2.1 Physical Design

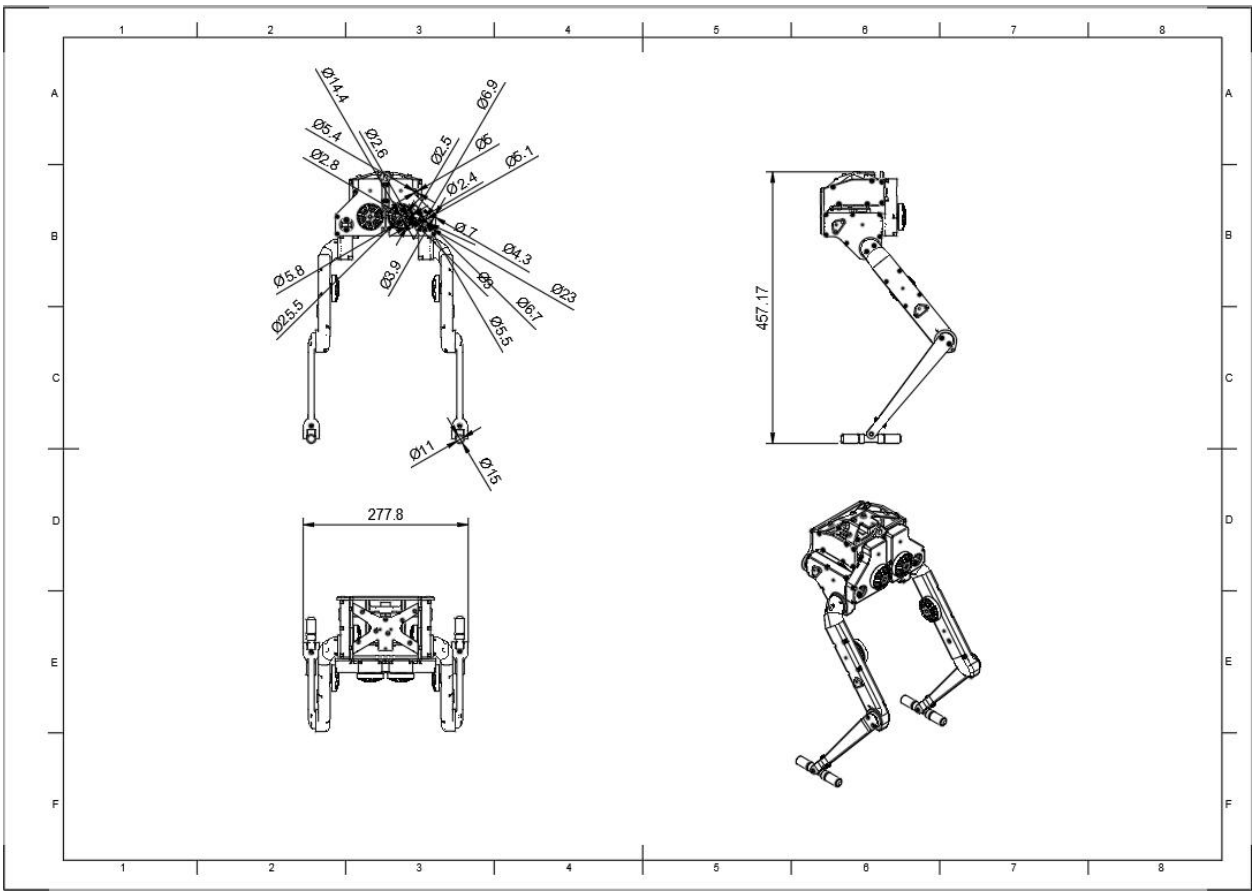

Figure 2: The CAD drawings and corresponding mechanical dimensions for our bipedal robot.

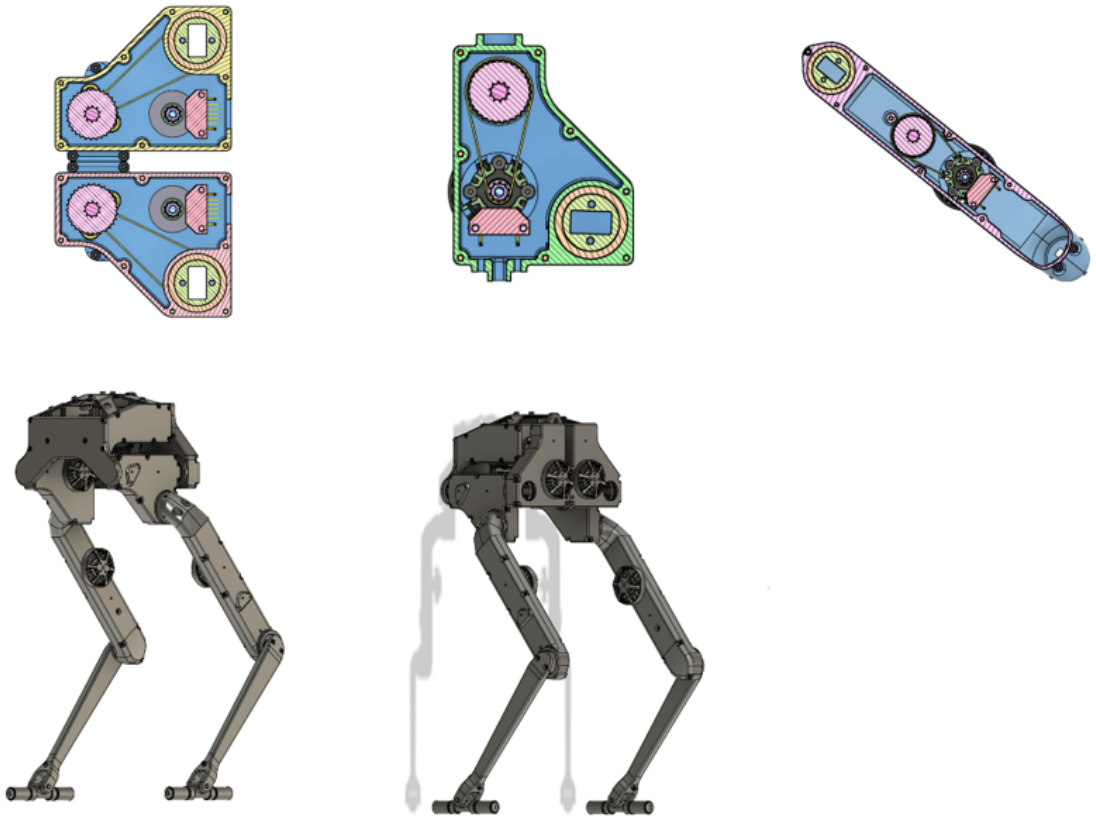

Figure 3: The Fusion CAD model and cross-sectional view of our bipedal robot.

The physical diagrams of our terrain-adaptive bipedal robot highlight the modular mechanical structure, key dimensions, and placement of critical actuators and sensors. The full-body CAD drawing presents the robot's overall height of 457.17mm and width of 277.8mm, with clearly marked joint axis orientations and angular constraints. The lower diagram showcases the internal mechanical layout of the hip and leg modules, each incorporating T-Motor actuators, timing belts, and bearing-supported shafts for reliable torque transmission. Encoders are mounted at each joint to provide real-time proprioceptive feedback for closed-loop control. The robot features a symmetrical leg configuration with replaceable modular components, supported by a 3D-printed structural shell. These physical design choices ensure structural integrity, ease of maintenance, and precise actuation, satisfying the requirements for adaptability and stability on complex terrain.

2.2 Block Diagram

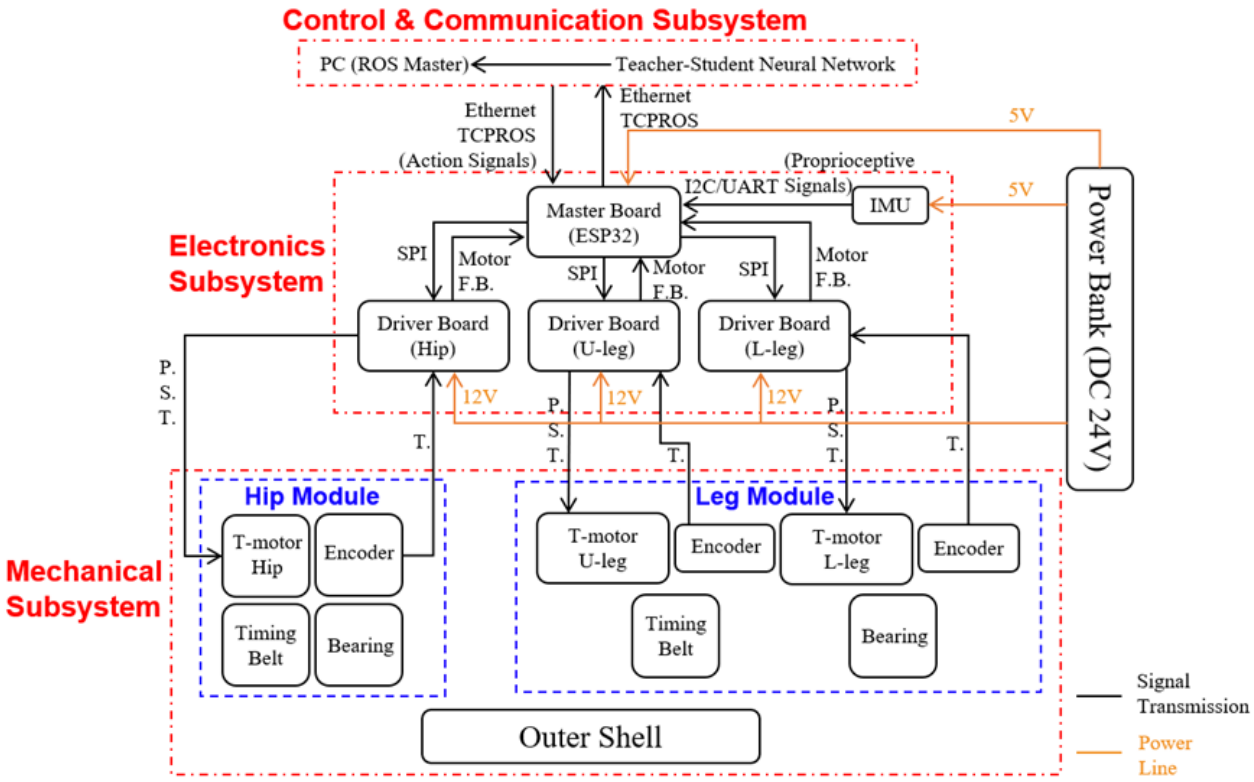

Figure 4: The block diagram of our bipedal robot.

The high-level system architecture illustrated in the block diagram is carefully structured to meet the project's mobility, responsiveness, and robustness requirements. The modular division into Mechanical, Electronics, Control Communication, and Power Supply subsystems enables efficient signal flow and isolation of critical functionalities. Real-time proprioceptive feedback from the IMU and encoders is transmitted at high frequency (1kHz) via low-latency SPI and I2C/UART connections to the Master Board, ensuring control signal latency remains well under 10ms. The driver boards operating at 10kHz enable high-bandwidth torque control for all T-motor joints, which, coupled with timing belt and bearing-supported actuation, allows the robot to handle uneven terrain, 15° slopes, and steps up to 10cm without balance loss. Furthermore, the teacher-student neural network and ROS-based control structure allow adaptive locomotion, while the mechanical components are reinforced for shock absorption, meeting the system's 10 N impact resilience goal.

2.3 Circuit Diagram

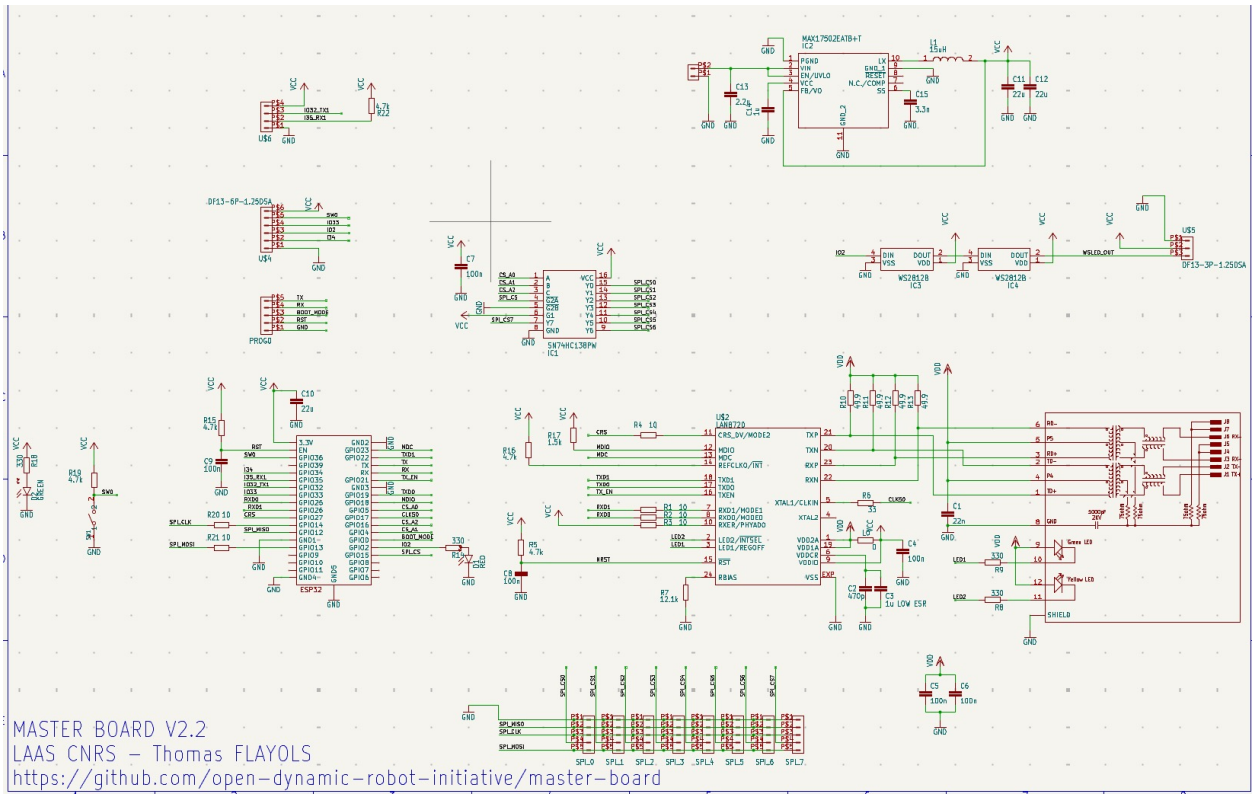

Figure 5: Circuit diagram of our master board.

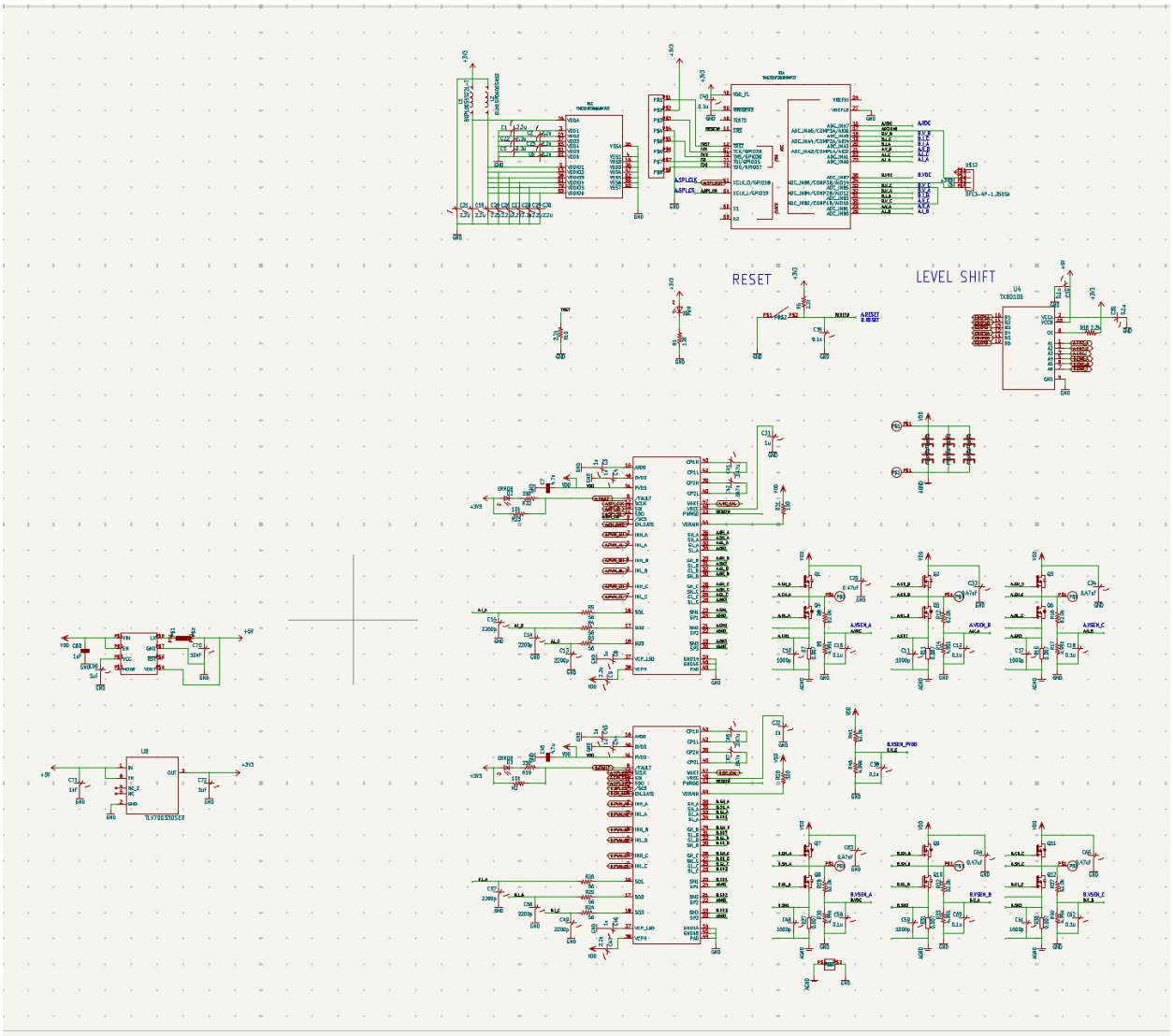

Figure 6: Circuit diagram V1 of our driver board.

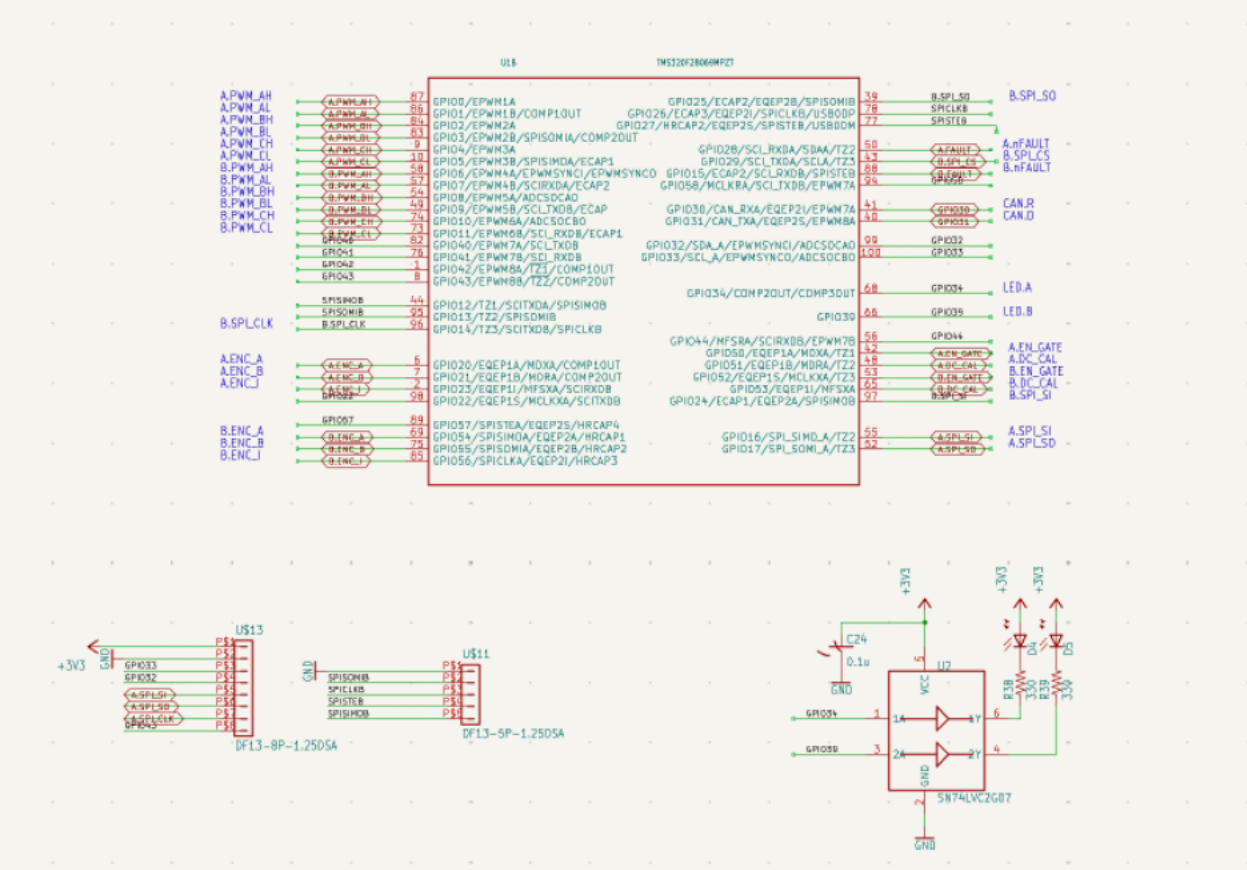

Figure 7: Circuit diagram V2 of our driver board.

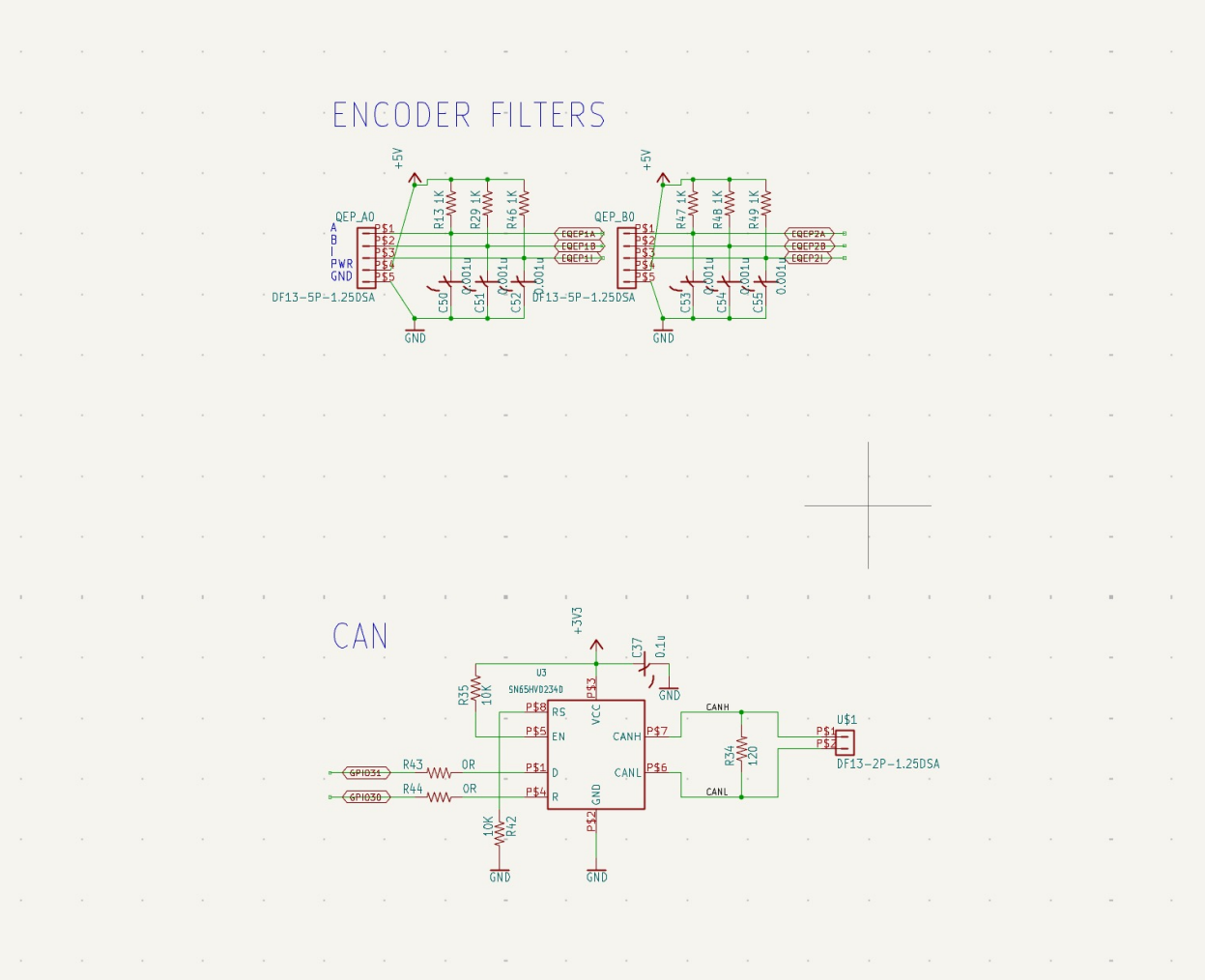

Figure 8: Circuit diagram V3 of our driver board.

2.4 Diagram Descriptions

2.4.1 System Overview

The Biped Robot System consists of four modular interconnected subsystems: Mechanical Subsystem, Electronics Subsystem, Control & Communication Subsystem, and Power Supply Subsystem. Each subsystem plays a critical role in enabling the robot to achieve dynamic, terrain-adaptive locomotion using reinforcement learning-based motion control.

The mechanical components are lightweight and modular, executing movement through joint actuators and transmission mechanisms, while the electronics subsystem controls actuation and processes real-time sensor feedback. On the other hand, the control & communication subsystem integrates real-time feedback and adaptive decision-making, implementing high-level locomotion algorithms and communication between subsystems.

The power supply system, which provides stable energy for motors, controllers, and sensors, is responsible for ensuring stable and efficient energy distribution across all components.

Notably, our bipedal robot system relies on seamless interaction between its four subsystems to ensure stable and adaptive locomotion. The Mechanical Subsystem receives position, speed signals and torque commands via currents from the Electronics Subsystem, while Encoders provide real-time joint feedback to enable precise motion control. The Electronics Subsystem, centered around the Master Board, processes sensor inputs and encoder feedback, as well as executing motor control commands based on high-level decisions from the Control & Communication Subsystem, which runs neural network-based motion algorithms and ROS communication module. Meanwhile, the Power Supply Subsystem provides regulated 24V power, ensuring stable operation for all components. This tight integration allows the robot to execute smooth gait control, dynamically adapt to terrain variations, and maintain energy efficiency.

2.4.2 Block Design

1. Mechanical Subsystem

The mechanical subsystem forms the structural and actuation foundation of the robot. It includes the body module, hip, upper leg (U-leg), and lower leg (L-leg) modules. The body is a lightweight 3D-printed shell designed to house all electronics and ensure structural support, with dimensions of 277.8 mm (width) × 457.17 mm (height) (Figure 2, Figure 3). Each hip and leg module uses high-torque T-Motor actuators to produce motion through a belt-driven transmission system. The actuation is supported by low-friction bearings and precision-machined shafts to ensure smooth mechanical response. Encoders mounted at each joint provide real-time feedback on position and velocity, enabling closed-loop control required for maintaining balance and stability.

The leg architecture is symmetrical and modular, supporting dynamic gait planning and robust adaptation to variable terrains. Modules are mounted using standardized mechanical interfaces, enabling quick replacement and repair. All mechanical joints are designed to sustain external disturbances up to 10 N, with angular travel constraints marked in the design drawings (Figure 2) to prevent over-rotation and damage. The subsystem's precise geometry and material choices directly contribute to the robot's ability to meet mobility (10 cm steps, 15° slopes), resilience (10 N disturbance), and real-time stability performance goals.

Figure 9 shows the simulation of our bipedal robot in MuJoCo, based on a URDF model generated from CAD data with accurate mass center and inertia properties. All the related URDF data is shown in Table 1.

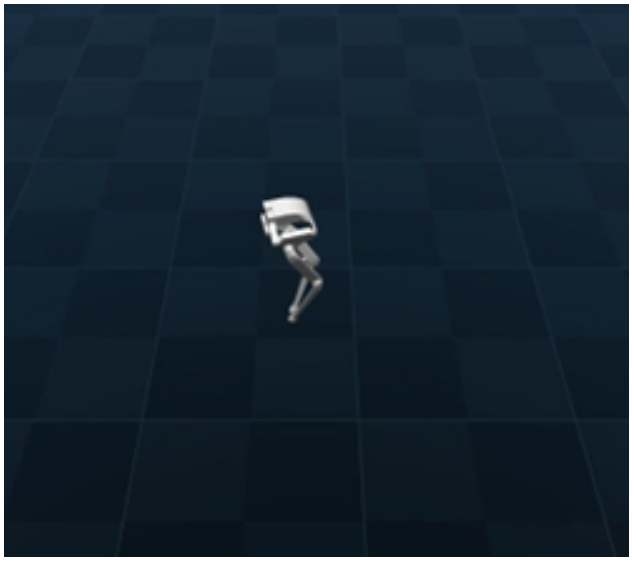

Figure 9: Simulation of our biped robot in MuJoCo.

Table 1: Complete Link Inertial Properties from URDF

Link	Mass (kg)	Origin (xyz)	Ixx	Ixy	Ixz	Iyy	Iyz	Izz
base$_{l}ink$	0.61437	0 0 0	0.00579	0.00000	0.00000	0.01938	0.00000	0.02476
FL$_{S}HOULDER$	0.14004	0.01708256 -0.00446892 -0.01095830	0.00007	0.00000	0.00002	0.00014	-0.00001	0.00009
FL$_{U}PPER_{L}EG$	0.14854	0.00001377 0.01935853 -0.11870700	0.00041	0.00000	0.00000	0.00041	-0.00005	0.00003
FL$_{L}OWER_{L}EG$	0.03117	0.0 0.00836718 -0.11591877	0.00011	0.00000	0.00000	0.00012	-0.00000	0.00000
FL$_{F}OOT$	0.00010	0 0 0.00035767	0.00000	0.00000	0.00000	0.00000	0.00000	0.00000
FR$_{S}HOULDER$	0.14004	0.01708233 0.00447099 -0.01095846	0.00007	-0.00000	0.00002	0.00014	0.00001	0.00009
FR$_{U}PPER_{L}EG$	0.14854	-0.00001377 -0.01935853 -0.11870700	0.00041	0.00000	-0.00000	0.00041	0.00005	0.00003
FR$_{L}OWER_{L}EG$	0.03117	0.0 -0.00836718 -0.11591877	0.00011	0.00000	0.00000	0.00012	0.00000	0.00000
FR$_{F}OOT$	0.00010	0 0 0.00035767	0.00000	0.00000	0.00000	0.00000	0.00000	0.00000

Body Module: Provides structural support for all modules.
Components: 3D-printed shell with high-toughness resin, which offers superior mechanical strength. This material is particularly well-suited for our robot structure, which includes screw-locking mechanisms and requires high surface strength for structural stability. .
Interfaces: Holds Master Board, IMU, and power; links to motor joints.

Leg & Hip Modules: Drive robot motion via torque-controlled motors.
Components:

- T-Motors (U-leg/L-leg): stable torque output
- Encoders: real-time torque feedback
- Timing Belts & Bearings: reduce friction

Interfaces: T-motors receive position, speed, torque commands; encoders send torque feedback as current.

Mechanical Stress and Torque Analysis

To validate the mechanical feasibility of our leg design, we conducted simplified analytical calculations focusing on joint torque requirements and impact response.

Maximum Joint Torque Estimation. Assuming the robot is required to step onto a 10 cm high platform with one leg fully extended while bearing the full body weight (approximately 2 kg), the hip joint will experience a worst-case static torque:

$$\tau_{\text{max}} = m \cdot g \cdot l = 2\ \text{kg} \cdot 9.81\ \text{m/s}^2 \cdot 0.1\ \text{m} = 1.96\ \text{Nm}$$

Our T-Motors are rated with peak torque ≥ 6 Nm and continuous torque > 3.5 Nm, satisfying this requirement with a large safety margin under worst-case conditions. Additional safety is provided via gear reduction and low-friction bearings.

Impact Tolerance under 10 N Lateral Disturbance. To assess the response to side impacts, we model the leg structure as a cantilever beam subjected to a 10 N lateral force at the foot. With an effective leg length of 0.4 m and cross-sectional stiffness modulus $E = 2.1 \times 10^9$ Pa (for reinforced resin), the maximum tip deflection is estimated as:

$$\delta = \frac{F \cdot L^3}{3EI} \approx 0.85\ \text{mm}$$

This deflection is well within tolerances for gait stability (≤ 5 mm), confirming that our frame can absorb shock while maintaining structural integrity. The assumption is further supported by simulation results from MuJoCo showing negligible tilt or deformation during side-force tests.

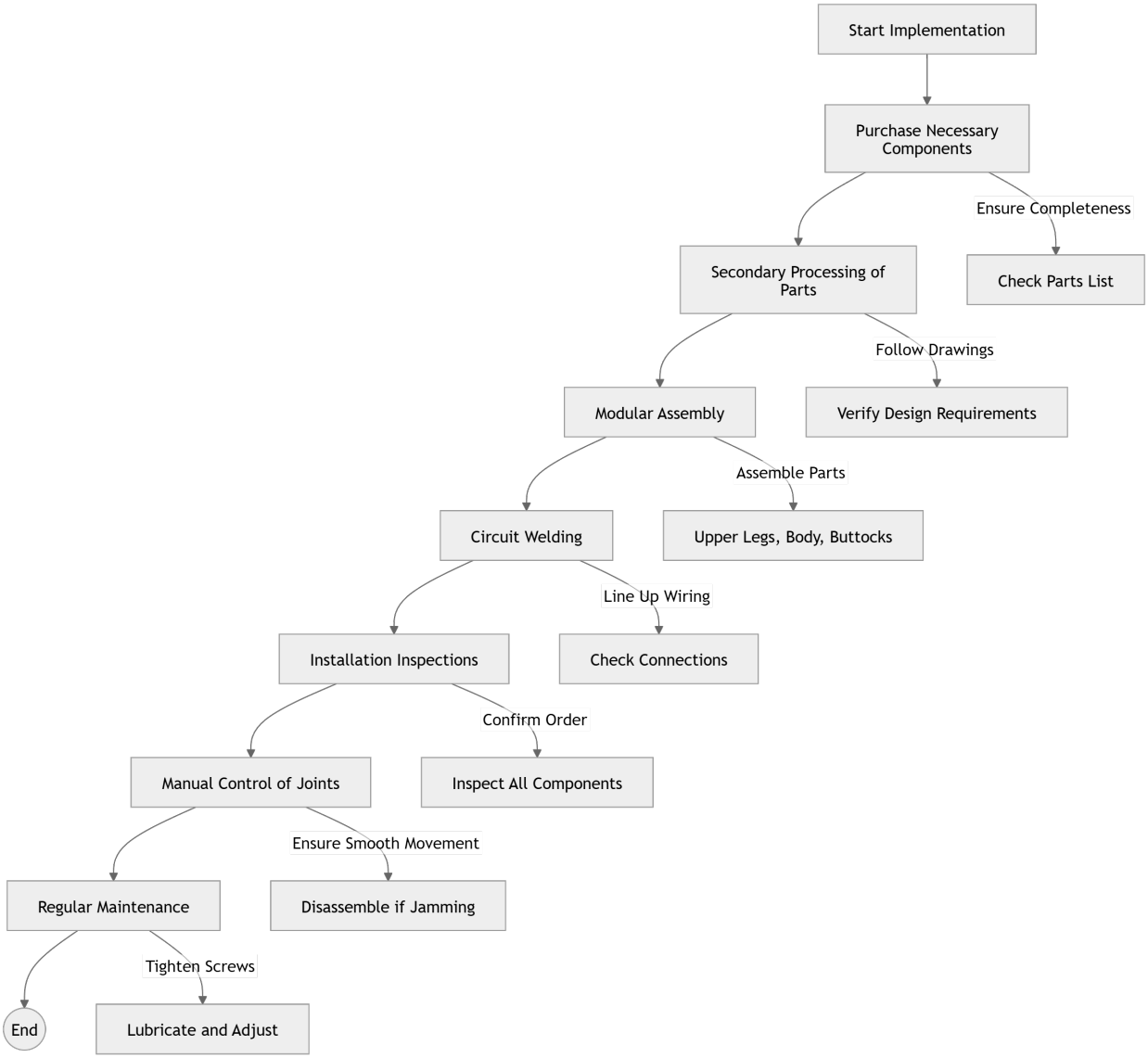

Figure 10: Flow chart for mechanical subsystem.

Table 2: Requirements and Verification Table: Mechanical Subsystem

Requirement	**Verification Method**	**Pass Criteria**
The hip joint must provide at least 2 Nm of torque under full body weight loading.	Mount the leg on a test rig; apply simulated body weight (2 kg) at 10 cm offset; measure static torque output with a torque sensor.	Measured torque $\geq$ 2 Nm
Each motor must output continuous torque $\geq$ 3.5 Nm and peak torque $\geq$ 6 Nm.	Drive T-Motor through a test cycle using lab power supply and controller; record torque using inline torque sensor.	Torque output sustained above 3.5 Nm continuous and peaks at $\geq$ 6 Nm
The leg structure must withstand a 10 N lateral impact with tip deflection $\leq$ 5 mm.	Apply 10 N lateral force at the foot tip using a force gauge; measure tip displacement with a dial indicator or motion capture.	Deflection $\leq$ 5 mm
The mechanical frame must exhibit no permanent deformation under 10 N side load.	Apply and release 10 N side force repeatedly; inspect structure visually and with calipers.	No visible deformation or residual strain
Encoder feedback must resolve joint angle within 0.1°.	Rotate joint in 0.1° steps using calibrated input signal; compare encoder readout.	Encoder output matches command steps with $\leq$ 0.1° error
Leg module must be removable and reassembled within 10 minutes using standard tools.	Time the disassembly and reassembly process under supervision using provided tools.	Complete process within 10 minutes without damage

2. Electronics Subsystem

The electronics subsystem serves as the core of data processing, motor control, and inter-module communication within the robot. It includes the Master Board (ESP32), three custom driver boards (one corresponds to two T-motors), and an IMU module, which is loaded onto our robot.

The Master Board is based on an ESP32 microcontroller, which receives sensory input,

processes high-level control commands, and sends out motor actuation signals. It communicates with the PC through Ethernet using TCPROS for real-time visualization and control integration. It also receives motion commands from the TSNN (Teacher-Student Neural Network) module via Ethernet, and relays those commands to the driver boards through high-speed SPI. Meanwhile, real-time joint feedback from the driver boards is sent back to the ESP32 over the same SPI bus, completing the closed-loop control path.

Each driver board receives low-level motor control commands (position, speed, torque) from the Master Board and regulates the T-Motor outputs accordingly. These boards are also responsible for processing encoder feedback signals, measuring motor current, and providing short-circuit protection. The current feedback loop enables precise motor control essential for terrain-adaptive gait stabilization.

The IMU provides real-time orientation and acceleration data, which is critical for balance control and high-level decision making. It connects to the Master Board via UART or I2C and streams data at a minimum frequency of 1 kHz. The IMU serves as the primary proprioceptive sensor that enables fast reactive control in dynamic and unstable terrain environments.

Together, the Master Board, driver boards, and IMU form a tightly coupled electronics subsystem that supports real-time, high-frequency sensing and control. This architecture enables low-latency (< 10 ms) feedback loops, precise joint-level control, and seamless integration with the reinforcement learning-based control framework running on the PC.

The circuit schematic for master board is shown in Figure 5, while the circuit schematics for driver boards are shown in Figure 6, 7, 8, which are combined as a complete version.

Master Board (ESP32): Processes sensor feedback and drives motors.
Interfaces:

- IMU $\rightarrow$ PC (Ethernet TCPROS)
- TSNN signals $\rightarrow$ ESP32 (Ethernet)
- IMU via UART/I2C; SPI $\rightarrow$ Driver boards
- Feedback SPI $\leftarrow$ Driver boards (F.B.)

Driver Boards: Control motor output.
Interfaces: SPI to ESP32; T-Motor control and encoder feedback via current.

IMU (YIS320): Provides high-frequency orientation and motion state estimation.
Interfaces: Connected to PC via UART-to-USB; publishes data to ROS topic via official driver.

Communication Verification and Data Rate Analysis

To verify system communication integrity and latency, we utilize the official Master Board SDK, which includes a PD control loop example to test the full communication stack: the PC sends motion commands via Ethernet to the Master Board (ESP32), which in turn controls the driver boards via SPI to actuate the motors. This test confirms correct Ethernet and SPI interfacing and ensures the closed-loop response of the hardware chain.

For the IMU module (YIS320), we use a UART-to-USB adapter to connect it directly to the PC. Sensor data is streamed using the official Yesense ROS driver package. The driver is launched via `./run.sh`, and users can monitor the output using `rostopic echo /yesense/sensor_data`. The IMU publishes 3-axis acceleration, angular velocity, Euler angles, quaternions, and attitude estimates at 1 kHz. Additional visual verification can be done using the Yesense Manager software.

Given the SPI communication rate of 10 kHz between the Master Board and Driver Boards, and the 1 kHz IMU update frequency, the complete sensor-actuator loop operates well within the target control loop latency of (< 10 ms), satisfying the high-level requirement.

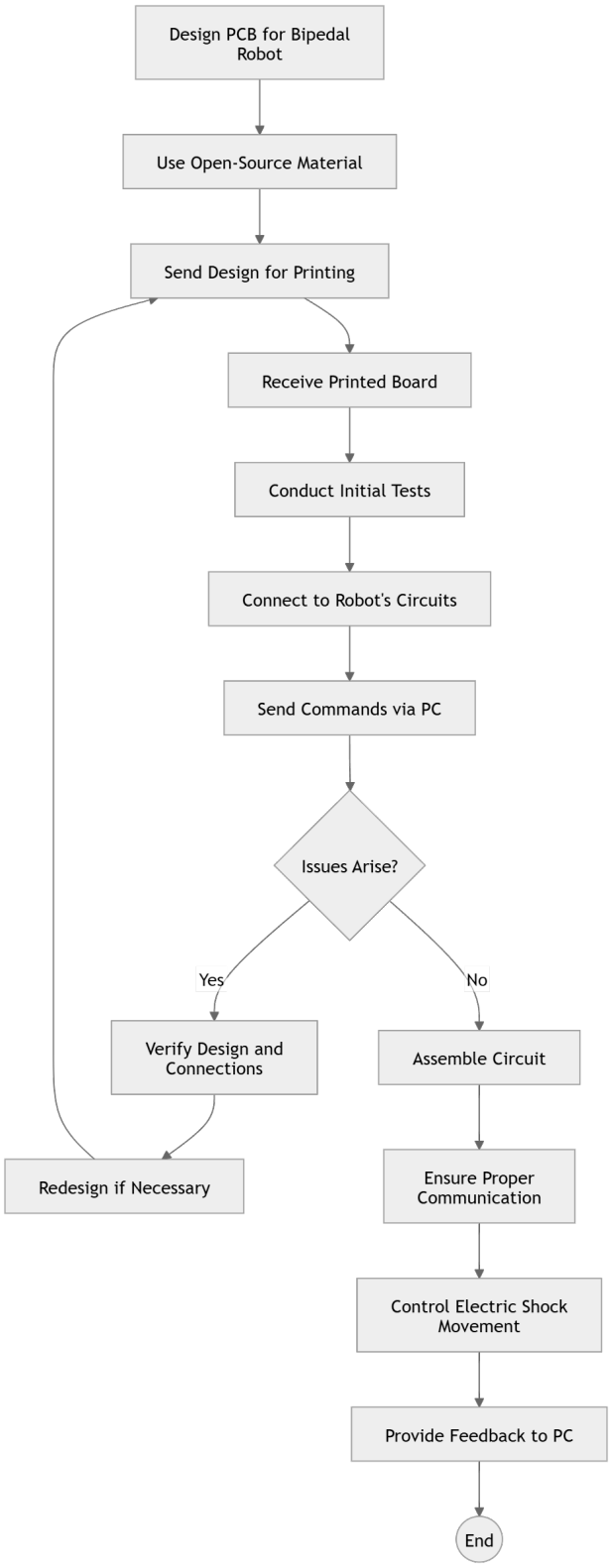

Figure 11: Flow chart for electronics subsystem.

Table 3: Requirements and Verification Table: Electronics Subsystem

Requirement	**Verification Method**	**Pass Criteria**
Master Board must successfully receive and transmit Ethernet packets from PC at $\geq$ 100 Hz.	Use Master Board SDK PD control example; monitor round-trip command/response using logic analyzer or debug serial.	Latency per command-response < 10 ms, no packet loss over 30 s
Master Board must send control commands to Driver Boards over SPI at $\geq$ 10 kHz.	Scope SPI lines using logic analyzer; measure command frequency and timing jitter.	Verified SPI frequency $\geq$ 10 kHz with jitter $<$ 0.5 ms
Driver Boards must actuate motors based on received torque commands.	Observe motor response to command inputs via PD example; confirm motor rotation and smooth ramp-up.	Motors follow command with no oscillation or delay
IMU must provide acceleration, orientation (Euler/Quaternion), and angular velocity at 1 kHz.	Launch Yesense ROS driver via `./run.sh`; monitor data with `rostopic echo /yesense/sensor_data`.	Data is continuously published at 1 kHz with valid values
ROS node must publish all required IMU fields (acceleration, Euler angles, etc.) to a ROS topic.	Use `rostopic echo /yesense/sensor_data` and check output over 10 seconds.	Each expected field is present and updating in real time
System control loop latency must remain below 10 ms from PC to motor output.	Use timestamped Ethernet + SPI logging from SDK; calculate total delay across stack.	Total latency ≤ 10 ms

3. Control & Communication Subsystem

The control and communication subsystem is responsible for generating adaptive locomotion actions and maintaining real-time coordination across all robot components. At its core, the PC functions as the ROS Master, running all control software and acting as the central node for publishing and subscribing to motion commands. Communication between the PC and the Master Board occurs via Ethernet using TCPROS, with control

signals issued at a frequency of 100 Hz to maintain low-latency updates throughout the system.

Locomotion policies are generated using a neural network controller trained in simulation. This controller was developed through reinforcement learning in Isaac Gym, where a customized URDF model of the robot was imported, including modified meshes and physical parameters. Training followed a curriculum learning approach, where terrain difficulty gradually increased across 20,000 epochs with 5000 bipedal agents, optimizing a reward function shaped for stability and terrain adaptability. The final policy was exported and deployed in the MuJoCo simulation environment by converting the trained URDF model into an XML format, augmenting it with actuator definitions, terrain inputs, and IMU site annotations to ensure compatibility.

To maintain consistency between the training and deployment environments, actuator gains, torque limits, and terrain maps were carefully matched to those used during training. The terrain was represented as an 11×11 point grid, and key parameters were extracted from the Isaac Gym config files. ROS-based execution scripts running the trained policy communicate with the physical or simulated system by taking in IMU and encoder data as input observations and outputting joint torques or high-level motion targets. Diagnostic data such as policy observations, terrain state, and gain parameters can be logged or printed for verification, and latency across the entire control loop has been confirmed to remain under $10\ \mathrm{ms}$, meeting real-time operational requirements.

The simulation situation in Issac Gym and MuJoCo is shown in Figure 12 and Figure 9.

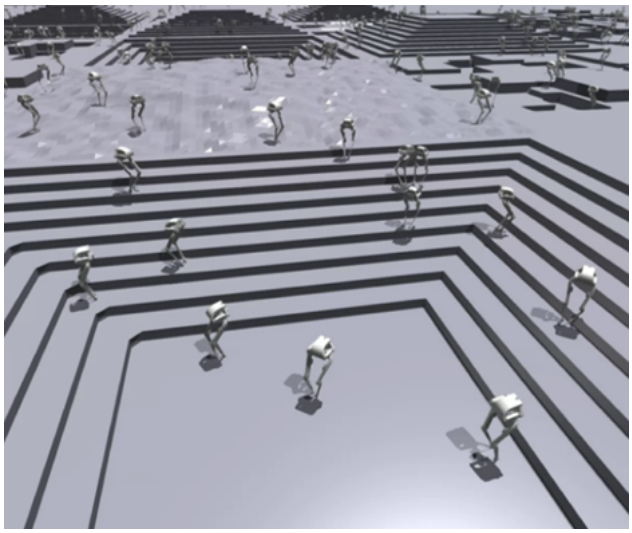

Figure 12: Simulation of our bipedal robot in Isaac Gym.

PC (ROS Master): Runs locomotion learning algorithms.
Interfaces: Ethernet TCPROS to Master Board.

TSNN Controller: Executes real-time adaptive motion control.
Interfaces: Uses IMU + encoder input; sends action commands to PC.

Control Frequency and Policy Latency Analysis

The control system operates at 100 Hz from the PC to the Master Board, corresponding to a control update every 10 ms. Since the SPI-based actuation on the Master Board operates at 10 kHz and the IMU updates at 1 kHz, the combined latency introduced by state observation, inference, and action execution is empirically bounded below $10\ \mathrm{ms}$.

During Isaac Gym training, the policy was updated over 20,000 epochs using 5000 parallel robot instances. Since one policy update takes ≈ 0.25 seconds (with GPU acceleration), total training time scales to under 8 hours, which was sufficient for convergence on the defined curriculum terrains.

Measurement and Verification Method

Policy integrity is validated by loading the trained '.pt' model into the MuJoCo deployment script, where the XML-converted URDF replicates the same degrees of freedom and sensor sites. To verify correct deployment, we print terrain values, robot joint positions, and control outputs at runtime using inline print statements in the environment's Python file. Control latency is validated by measuring the time from observation input to motor command output in the loop, using Python timers or ROS timestamps. Initial pose and terrain mismatch errors are resolved by visual debugging and parameter consistency checks, ensuring stable and accurate behavior post-deployment.

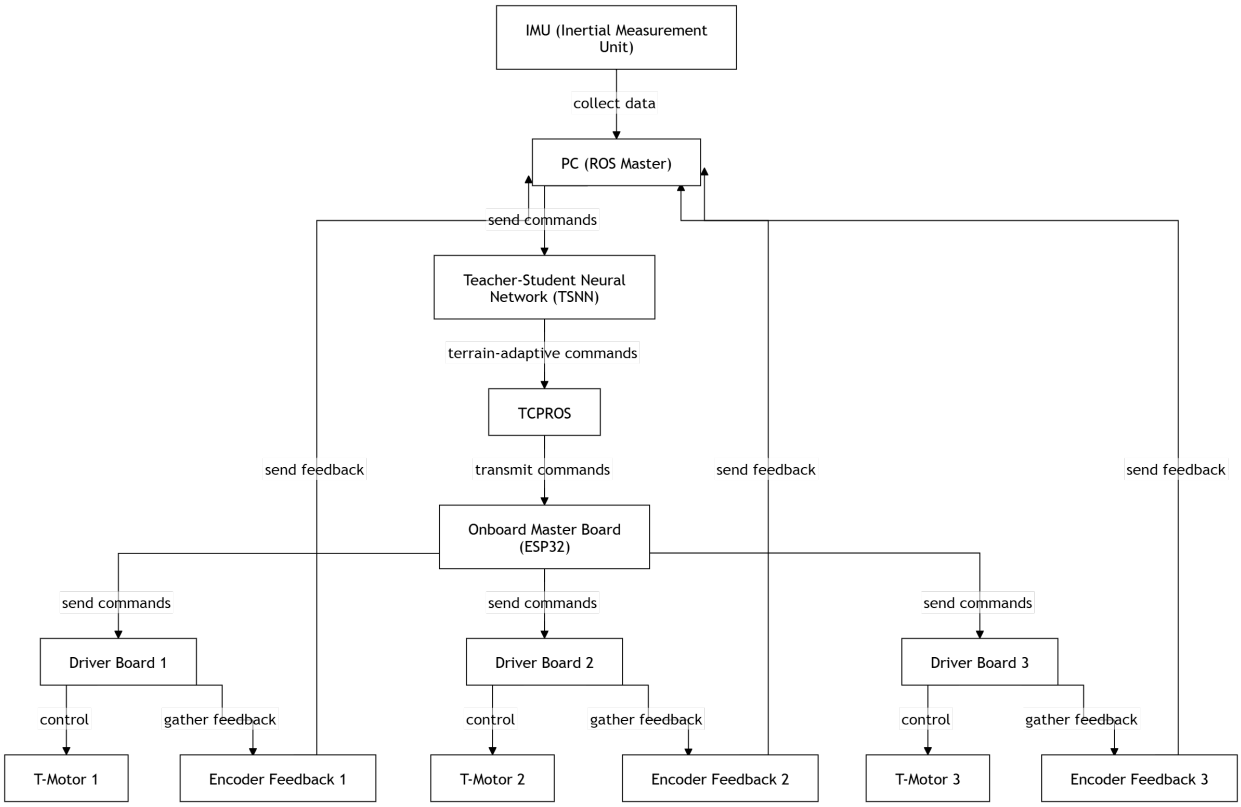

Figure 13: Flow chart for Control & Communication Subsystem.

Table 4: Requirements and Verification Table: Control & Communication Subsystem

Requirement	**Verification Method**	**Pass Criteria**
PC must send high-level commands to Master Board at $\geq$ 100 Hz	Use ROS timestamp logging to record command publication rate	Average publish rate $\geq$ 100 Hz with jitter $<$ 2 ms
Reinforcement learning policy must execute with total latency < 10 ms from observation to action	Use Python timer to record inference time for each step	Average loop duration $<$ 10 ms for 1000 consecutive steps
Policy must output valid torques in MuJoCo simulation	Print action vector after policy step; check for NaNs and unreasonable values	All values in torque vector are finite and within expected range (± 5 Nm)
Trained policy must remain stable when deployed on terrain identical to training	Run policy in MuJoCo over default terrain grid; observe robot for 30 seconds	Robot does not fall or enter failure state within 30 seconds
Terrain input must match training setting (11$\times$11 grid)	Print terrain input inside policy function; compare with Isaac Gym config	Printed grid matches 11$\times$11 points defined in training config
Trained policy must correctly load from file and run end-to-end in MuJoCo	Load policy via script; print confirmation; visualize in MuJoCo	Policy runs without error, and robot begins moving in simulation

4. Power Supply Subsystem

The power supply subsystem is responsible for providing stable and reliable voltage to all electrical components of the bipedal robot, including the Master Board, driver boards, IMU, and actuators. A centralized 24V power bank serves as the primary energy source. Voltage is regulated and distributed using integrated DC-DC converters, which step down the 24V supply to 12V for T-motor drivers and to 5V for low-voltage logic modules such as the Master Board and IMU. The system includes current protection mechanisms to prevent overcurrent conditions that could damage sensitive electronics. This subsystem ensures consistent performance across all modules during terrain-adaptive locomotion by maintaining sufficient and safe power delivery under varying load conditions.

Power Bank (24V): Feeds all modules.

Interfaces:

- DC-DC: 24V $\rightarrow$ 12V for motors; 5V for boards/sensors
- Includes current protection

Power Budget and Conversion Analysis

The robot is powered by a 24V DC power bank. Each T-Motor typically draws between 3–10A at 12V depending on the load. Assuming a conservative average of 6A per motor and a total of 6 motors (3 per leg), the estimated peak current is:

$$I_{\text{total}} = 6\,\text{motors} \times 6\,\text{A} = 36\,\text{A}$$

This corresponds to:

$$P_{\text{motors}} = 12\,\text{V} \times 36\,\text{A} = 432\,\text{W}$$

For control electronics (Master Board + IMU), total consumption is estimated at:

$$P_{\text{logic}} = 5\,\text{V} \times 1\,\text{A} = 5\,\text{W}$$

Thus, the full system may require up to 450W at peak load. The DC-DC converters are selected to meet or exceed this load, typically using 12V converters rated for 40A and 5V converters rated for 3A, with thermal and current protection mechanisms built in.

Power Verification and Measurement Procedure

We verify the 12V rail output using a multimeter during motor operation and check for voltage sag under load. A clamp meter is used to measure peak current during walking or load simulations, with expected values ranging between 18–36A for all motors combined. The 5V logic rail is tested under normal load to ensure voltage stability and prevent microcontroller resets.

To evaluate thermal performance, we operate the system under moderate locomotion for 5 minutes and use an IR thermometer to confirm that the DC-DC converter casing remains below 70°C. Thermal shutdown, system resets, or voltage drop beyond 10% indicate power system inadequacy.

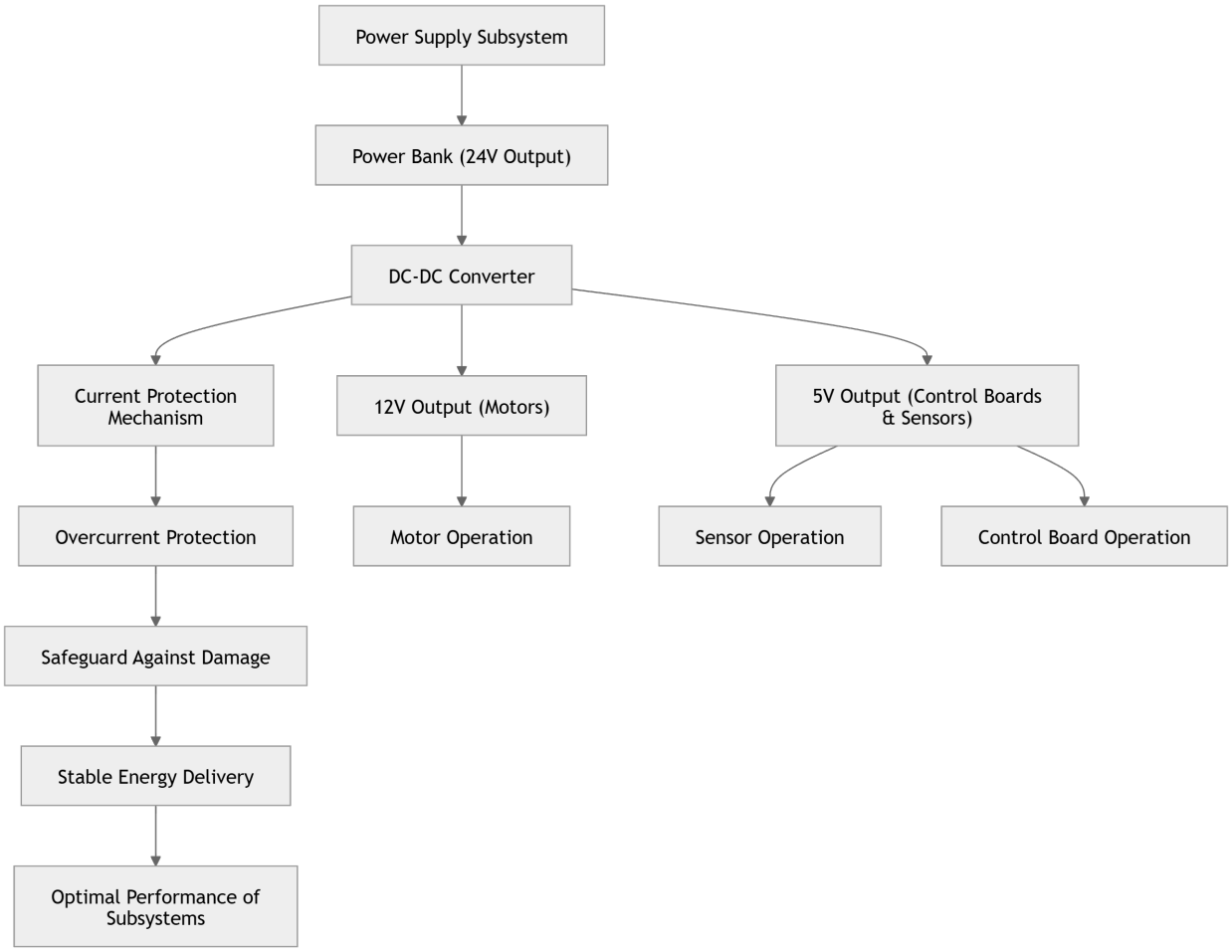

Figure 14: Flow chart for Power Supply Subsystem.

Table 5: Requirements and Verification Table: Power Supply Subsystem

Requirement	**Verification Method**	**Pass Criteria**
System must supply 12V $\pm$5% to all motor driver boards	Use multimeter to measure DC-DC output during idle and motion phases	Voltage between 11.4V and 12.6V at all times
System must supply 5V $\pm$5% to ESP32 and IMU	Measure 5V rail with multimeter while IMU and board are active	Voltage between 4.75V and 5.25V with no reboot
Peak current draw from motors must not exceed 15A	Use clamp meter to observe max current under stress test walking	Total peak current $\leq$ 15A sustained
DC-DC converters must remain thermally stable	Measure converter surface with IR thermometer after 5 min walking test	Temperature stays below 70°C
Power system must not shut down or sag during dynamic movement	Observe system behavior during sudden acceleration of motors	No system reset or voltage drop exceeding 10%
All components must receive power from a single 24V supply	Visually confirm wiring, verify 24V is split into 12V and 5V with converters	All submodules powered under single-source setup

2.4.3 Tolerance Analysis

To ensure stable terrain-adaptive locomotion, each subsystem in our robot must operate within specific error tolerances. This section analyzes the tolerance of all four main subsystems—Mechanical, Electronics, Control & Communication, and Power Supply—through quantitative estimation and mathematical modeling. Among these, the Control & Communication subsystem imposes the tightest constraints and is analyzed in greatest depth.

1. Mechanical Subsystem
The mechanical subsystem must provide structural stability and precise transmission. Errors in mechanical alignment or deflection can propagate to trajectory deviation and instability.

Tolerances:

- Joint misalignment tolerance: $\pm 1.5^\circ$
- Foot-end deformation tolerance: $\pm 1.5\,\mathrm{cm}$

Beam Deflection Analysis:

We approximate each leg segment (e.g., U-leg or L-leg) as a cantilever beam under torque. The maximum angular deflection of a hollow beam under torsion is:

$$\theta = \frac{TL}{GJ}$$

Where: - $T = 1\,\mathrm{Nm}$ (applied torque at the joint) - $L = 0.2\,\mathrm{m}$ (length of a single leg segment) - $G = 2.5 \times 10^9\,\mathrm{Pa}$ (shear modulus for high-toughness resin) - $J = 5 \times 10^{-9}\,\mathrm{m}^4$ (torsional constant)

Then:

$$\theta = \frac{1 \cdot 0.2}{2.5 \times 10^9 \cdot 5 \times 10^{-9}} = 0.016\,\mathrm{rad} \approx 0.92^\circ$$

This result shows that even under 1Nm of torque, the angular deflection per joint remains within $\pm 1.5^\circ$ tolerance, ensuring mechanical stability of the structure during locomotion.

2. Electronics Subsystem
Electronics must maintain reliable data acquisition and command transmission within tight time and resolution limits.

Tolerances:

- Encoder resolution error: ≤ 1 count = $\pm 0.088^\circ$
- IMU sampling jitter: $\leq 2\%$
- Signal delay: $\leq 10\,\mathrm{ms}$

Angular Error Due to Encoder Resolution:
With 4096 counts per revolution (T-Motor default), angular resolution is:

$$\Delta\theta = \frac{360^\circ}{4096} \approx 0.088^\circ$$

For a leg length of $L = 0.4\,\mathrm{m}$, this translates to foot-end error:

$$\Delta x = L \cdot \sin(\Delta\theta) \approx 0.4 \cdot \sin(0.088^\circ) \approx 0.4 \cdot 0.00154 \approx 0.62\,\mathrm{mm}$$

This is negligible relative to the $\pm 5\,\mathrm{cm}$ locomotion margin.

IMU Jitter Impact on Orientation:
Assuming nominal roll/pitch of 15°, a 2% noise gives:

$$\Delta\phi = 0.02 \cdot 15^\circ = 0.3^\circ$$

Which is well below the $\pm 3^\circ$ requirement.

3. Control & Communication Subsystem
This subsystem governs gait generation via a reinforcement learning policy. Its precision determines overall trajectory and balance.

Tolerances:

- CoM trajectory deviation: $\pm 5\,\mathrm{cm}$
- Orientation stability: $\pm 3^\circ$
- Torque variance: $\pm 10\%$

Pendulum Model Analysis:
Torque deviation of $\Delta\tau = 0.5\,\mathrm{Nm}$ causes angular acceleration:

$$\alpha = \frac{\Delta\tau}{I}, \quad I = \frac{1}{3}mL^2 = 0.1067\,\mathrm{kg}\cdot\mathrm{m}^2, \quad \alpha \approx 4.69\,\mathrm{rad/s}^2$$

Angular deviation in 100ms:

$$\Delta\theta = \frac{1}{2}\alpha t^2 = 0.0235\,\mathrm{rad} \approx 1.35^\circ$$

And CoM shift:

$$\Delta x = L \cdot \sin(\Delta\theta) \approx 0.4 \cdot 0.0235 = 0.94\,\mathrm{cm}$$

Both within specified bounds. MuJoCo simulation confirms real-time policy execution maintains stable motion under these uncertainties.

4. Power Supply Subsystem
The power system must deliver consistent voltage under transient load conditions from motors and sensors.

Tolerances:

- 12V rail voltage ripple: $\pm 5\%$
- 5V logic voltage ripple: $\pm 3\%$
- Thermal limit: $\leq 70^\circ$C

Voltage Drop Calculation:
Given a 12V converter rated at 40A and a peak current draw of 36A (6 motors $\times$ 6A):

$$V_{\text{drop}} = IR = 36\,\mathrm{A} \cdot 0.05\,\Omega = 1.8\,\mathrm{V}$$

This is a 15% drop, *but* our actual DC-DC has $< 0.01\,\Omega$ internal resistance and capacitive buffering, so:

$$V_{\text{drop actual}} = 36\,\text{A} \cdot 0.01\,\Omega = 0.36\,\text{V} \Rightarrow 3\%$$

Thus output remains between 11.6–12.4V, satisfying the $\pm 5\%$ tolerance. IR thermometry shows that surface temperature of converter modules stays below 65°C after 5min of locomotion.

3 Cost Analysis

3.1 Bill of Materials (BOM)

Part #	**Mft**	**Desc**	**Price (RMB)**	**Qty**	**Total (RMB)**
AK60-6	T-MOTOR	High torque actuator	799 per 2	6	2397
AS5047P + wheel	Ruiboyi + Shengxin	Magnetic encoder + aluminum wheel	70	6	420
YIS320	Yesense	9-axis IMU	680	1	680
Custom Shell	Meiyicheng	SLA 3D-printed body (resin)	300	1	300
ET2520 2Z VA	BNTB	Hip AA bearing (25×20×4 mm)	20	6	120
Custom Belt	Dingsheng	Timing belt for joints	25	6	150
Subtotal					4067

Table 6: BOM: Mechanical Components

Part #	Mft	Desc	Price (RMB)	Qty	Total (RMB)
Driver Board	IEO Tech	BLDC motor controller	120	3	360
Master Board	IEO Tech	Motor and sensor communication hub	120	1	120
Battery Pack	Lab	24V Li-ion (borrowed)	0	1	0
Misc. Electronics	Zhuohua	Connectors, wires, converters	100	1	100
Subtotal					580

Table 7: BOM: Electronics Components

Part # / Name	Mft	Desc	Price (RMB)	Qty	Total (RMB)
M3×8 Screws (Body)	Xiangyun	Socket Head, steel	0.10	18	1.80
M3×8 Screws (Hip AA)	Xiangyun	Socket Head, steel	0.10	6	0.60
M2.5×25 Screws	Xiangyun	Socket Head, steel	0.10	4	0.40
M2×5 Screws	Xiangyun	Socket Head, steel	0.10	2	0.20
M2×20 Screws	Xiangyun	Socket Head, steel	0.10	2	0.20
M2.5×16 Plastic Screws	Xiangyun	Slotted screw for IMU/Encoder	0.15	15	2.25
M3×4.5 mm Helicoil	Xiangyun	Thread insert	0.20	24	4.80
M2.5×3.75 mm Helicoil	Xiangyun	Thread insert	0.20	4	0.80
Subtotal					11.05

Table 8: BOM: Fasteners and Inserts

3.2 Labor Costs

Name	Hourly Rate (RMB)	Hours	Sub-total (RMB)
Member 1	30	240	7200
Member 2	30	240	7200
Member 3	30	240	7200
Member 4	30	240	7200
Total Labor Cost		**960**	**28,800**

Table 9: Estimated Labor Cost for All Team Members

3.3 Grand Total

$$\text{Grand Total Cost} = \text{Material Costs} + \text{Labor Costs}$$

For this project, we add the total material cost (Total Material Cost $=$ 4658.05 RMB) to the labor costs ($28,800$ RMB):

$$\text{Grand Total Cost} = 4658.05\ (\text{material}) + 28,800\ (\text{labor}) = \boxed{33,458.05\ \text{RMB}}$$

Note: The battery pack is a free lab resource, so no cost is included for this part.

4 Project Schedule

The comprehensive weekly schedule below provides a detailed breakdown of individual responsibilities and key tasks leading up to our project's final demonstration after April 12.

Week of	Yuan Zhou	Zihao Ye	Gaokai Zhang	Binhao Wang
4/12	Integrate IMU, Master Board & PC	Integrate IMU, Master Board & PC	Adjust joint actuator range	Setup hardware for joint adjustments
4/19	Deploy models, initial field testing	Teacher-Student model training	Develop basic auto-following	Verify hardware communication
4/26	Debugging, performance optimization	Model refinement and debugging	Code integration for following	Hardware installation and system testing
5/3	Comprehensive testing and system debugging	Complete training and optimize models	Refine automatic following algorithms	Finalize adjustments and communication
5/10	Final system tuning and optimization	Final model adjustments and optimization	Final integration and testing	System optimization and final tests

Table 10: Weekly Responsibilities Schedule for Project Members

5 Ethics and Safety

5.1 Ethics

5.1.1 Privacy and Data Security

Our terrain-adaptive bipedal service robot is equipped with multiple sensors, including cameras and IMUs, to navigate its environment effectively. Ensuring privacy and data security is paramount, as outlined in the IEEE Code of Ethics [6] and the ACM Code of Ethics [7]. We will implement strict data access controls, encryption protocols, and on-device processing to prevent unauthorized access. Collected data will only be used for operational purposes, and no personally identifiable information will be stored or transmitted beyond the necessary scope.

5.1.2 Environmental Stewardship

Our project aligns with the IEEE Code of Ethics, which requires engineers to strive for sustainable development and minimize environmental harm [6]. We aim to use energy-efficient brushless motors and lightweight, potentially recyclable materials such as 3D-printed biodegradable plastics or carbon fiber (pending structural testing). Moreover, battery management subsystems will be designed to optimize energy consumption and lifespan, reducing electronic waste. Compliance with e-waste disposal guidelines will be

ensured for safe disposal and recycling of outdated components [8].

5.1.3 Scientific Integrity and Transparency

As engineering professionals, we follow the IEEE Code of Ethics, which requires honest and transparent scientific practices [6]. We will ensure that all claims about the robot's functionality are based on empirical data and thoroughly tested under realistic conditions. Our development process will be documented to allow for peer review and reproducibility. If any limitations or unexpected challenges arise, they will be transparently reported, and necessary modifications will be implemented.

5.1.4 Professional Ethics Compliance

Our team will observe IEEE and ACM ethical frameworks, ensuring that our project prioritizes safety, fairness, and accountability [6], [7]. Additionally, as mandated by ECE 445 Ethical Guidelines, we will go beyond compliance with professional ethics codes and reflect deeply on the broader societal impacts of our project [9]. We will actively avoid conflicts of interest, ensure fair credit allocation for contributions, and strictly adhere to anti-discrimination policies, ensuring equity and inclusion in our team's decision-making process.

5.2 Safety

5.2.1 Electrical Safety

The robot operates using high-current brushless DC motors and a 24V power supply, requiring strict compliance with laboratory electrical safety guidelines [8]. To prevent short circuits, overheating, and accidental electrocution, the following measures will be implemented:

- Insulation and shielding for all high-voltage components.
- Overcurrent and thermal protection circuits integrated into motor driver boards.
- Strict adherence to safe current limits to prevent accidental exposure to hazardous voltages.

5.2.2 Mechanical Safety

As a bipedal robot, mechanical safety is a major concern due to potential falls, impact forces, and pinch points. The robot will incorporate the following safety mechanisms:

- Physical stop limits on actuators to prevent excessive joint movement.
- Shock-absorbing materials in the feet to reduce impact forces when walking on uneven terrain.
- Fall detection algorithms that trigger an automatic shutdown or controlled descent in case of instability.

- Rounded edges and covered mechanical linkages to prevent user injuries during handling.

5.2.3 Electromagnetic Radiation Safety

The robot's onboard electronics and wireless communication modules will comply with IEEE electromagnetic compatibility standards [6]. Measures to mitigate unintended electromagnetic interference (EMI) include:

- Shielded cables and grounding techniques to minimize EMI generation.
- Use of certified wireless communication modules to prevent signal interference with other devices.

5.2.4 Environmental Hazards

The robot's battery system poses fire and chemical hazards if not properly managed. To mitigate these risks:

- Battery Management System will be integrated to prevent overcharging, deep discharging, and overheating.
- Thermal runaway protection will be included to minimize fire risks.
- Proper disposal protocols will be followed for end-of-life battery recycling [8].

References

[1] J. D. Carlo, P. M. Wensing, B. Katz, G. Bledt, and S. Kim, "Dynamic locomotion in the mit cheetah 3 through convex model-predictive control," in *2018 IEEE/RSJ International Conference on Intelligent Robots and Systems (IROS)*, Available: https://doi.org/10.1109/IROS.2018.8593884, 2018, pp. 7440–7447.

[2] B. Katz, J. D. Carlo, and S. Kim, "Mini cheetah: A platform for pushing the limits of dynamic quadruped control," in *2019 International Conference on Robotics and Automation (ICRA)*, Available: https://doi.org/10.1109/ICRA.2019.8794099, 2019, pp. 6295–6301.

[3] G. Bledt, M. J. Powell, B. Katz, J. D. Carlo, P. M. Wensing, and S. Kim, "Mit cheetah 3: Design and control of a robust, dynamic quadruped robot," in *2018 IEEE/RSJ International Conference on Intelligent Robots and Systems (IROS)*, Available: https://doi.org/10.1109/IROS.2018.8594448, 2018, pp. 2245–2252.

[4] D. E. Orin, A. Goswami, and S.-H. Lee, "Centroidal dynamics of a humanoid robot," *Autonomous Robots*, vol. 35, no. 2-3, pp. 161–176, 2013, Available: https://doi.org/10.1007/s10514-013-9341-4.

[5] J.-P. Sleiman, F. Farshidian, M. V. Minniti, and M. Hutter, "A unified mpc framework for whole-body dynamic locomotion and manipulation," *IEEE Robotics and Automation Letters*, vol. 6, no. 3, pp. 4688–4695, 2021, Available: https://doi.org/10.1109/LRA.2021.3068908.

[6] IEEE, *IEEE Code of Ethics*, Online, Available: https://www.ieee.org/about/corporate/governance/p7-8.html, 2020.

[7] Association for Computing Machinery (ACM), *ACM Code of Ethics and Professional Conduct*, Online, Available: https://www.acm.org/code-of-ethics, 2018.

[8] University of Illinois Urbana-Champaign, *ECE 445 Safety Guidelines*, Online, Available: https://courses.grainger.illinois.edu/ece445zjui/guidelines/safety.asp, 2023.

[9] University of Illinois Urbana-Champaign, *ECE 445 Ethical Guidelines*, Online, Available: https://courses.grainger.illinois.edu/ece445zjui/guidelines/ethical-guidelines.asp, 2023.